A Face-on Accretion System in High Mass Star-Formation: Possible Dusty Infall Streams within 100 Astronomical Unit

**Kazuhito Motogi[1], Tomoya Hirota[2,3], Kazuo Sorai[4],[5],
Yoshinori Yonekura[6], Koichiro Sugiyama[2], Mareki Honma[7],
Kotaro Niinuma[1], Kazuya Hachisuka[7], Kenta Fujisawa[8] and
Andrew J. Walsh[9]**

[1]Graduate School of Sciences and Technology for Innovation,Yamaguchi University,
Yoshida 1677-1, Yamaguchi 753-8512, Japan
email: kmotogi@yamaguchi-u.ac.jp

[2]Mizusawa VLBI Observatory, National Astronomical Observatory of Japan,
Osawa 2-21-1, Mitaka, Tokyo 181-8588, Japan

[3]Department of Astronomical Sciences, SOKENDAI
(The Graduate University for Advanced Studies),
Osawa 2-21-1, Mitaka, Tokyo 181-8588, Japan

[4]Department of Physics, Faculty of Science, Hokkaido University,
Sapporo 060-0810, Japan

[5]Department of Cosmosciences, Graduate School of Science, Hokkaido University,
Sapporo 060-0810, Japan

[6]Center for Astronomy, Ibaraki University,
2-1-1 Bunkyo, Mito, Ibaraki 310-8512, Japan

[7]Mizusawa VLBI Observatory, National Astronomical Observatory of Japan,
Hoshigaoka 2-12, Mizusawa, Oshu, Iwate 023-0861, Japan

[8]The Research Institute for Time Studies, Yamaguchi University,
Yoshida 1677-1, Yamaguchi 753-8511, Japan

[9]International Centre for Radio Astronomy Research, Curtin University,
Bentley, WA 6102, Australia

Abstract. We report on interferometric observations of a face-on accretion system around the high mass young stellar object, G353.273+0.641. The innermost accretion system of 100-au radius was resolved in a 45-GHz continuum image taken with the Jansky Very Large Array. Our SED analysis indicated that the continuum could be explained by optically-thick dust emission. 6.7 GHz CH_3OH masers associated with the same system were also observed with the Australia Telescope Compact Array. The masers showed a spiral-like, non-axisymmetric distribution with a systematic velocity gradient. The line-of-sight velocity field is explained by an infall motion along a parabolic streamline that falls onto the equatorial plane of the face-on system. The streamline is quasi-radial and reaches the equatorial plane at a radius of 16 au. The physical origin of such a streamline is still an open question and will be constrained by the higher-resolution thermal continuum and line observations with ALMA long baselines.

Keywords. ISM: individual objects (G353.273+0.641) – molecules – masers – radio continuum: ISM – stars: formation

1. Introduction

G353.273+0.641 (hereafter G353), is a relatively nearby (1.7 kpc) high mass young stellar object (HMYSO) in the southern sky (Motogi *et al.* 2016). The bolometric

luminosity of $\sim 5 \times 10^3$ $L_\odot$ corresponds a B1-type ZAMS, implying a stellar mass of ~ 10 $M_\odot$ (Motogi *et al.* 2017). G353 is also known as a Dominant Blue-Shifted Maser (DBSM) source that is a class of 22 GHz H_2O masers showing a highly blue-shift dominated spectrum (Caswell & Phillips 2008). The line-of-sight (LOS) velocities of the maser typically range from -120 to -45 km s^{-1} and the systemic velocity (V_{sys}) is $\sim$-5.0 km s^{-1} in the case of G353 (e.g., Motogi *et al.* 2016). Caswell & Phillips (2008) proposed that DBSMs are candidates of HMYSOs with a face-on protostellar jet. The inclination angle of the jet, that was estimated by maser proper motions, is 8 – 17deg from the LOS (Motogi *et al.* 2016). G353 is, at present, the best candidate of a face-on HMYSO in the active accretion phase.

2. Observation

We have searched for a face-on accretion system associated with G353, via the highest-resolution (A-configuration) continuum imaging using the Jansky Very Large Array (JVLA). In addition to the 45 GHz data reported in Motogi *et al.* (2017), new 20 – 30 GHz continuum data were added. We also performed mapping observations of the associated 6.7 GHz class II CH_3OH maser (e.g., Caswell & Phillips 2008) by the Australia Telescope Compact Array (ATCA) in 6A configuration (see Motogi *et al.* 2017 for details).

3. Results

3.1. *Centimeter Continuum*

Figure 1 shows a 45-GHz continuum image taken by the JVLA in A-configuration (Motogi *et al.* (2017)). A very compact continuum source was detected at the center of the bipolar H_2O maser jet. The source was resolved along the minor axis of the synthesized beam (E-W direction). Total flux of 3.5 mJy and the size of the deconvolved Gaussian (FWHM: $0''.123 \times 0''.073$) indicate the averaged brightness temperature T_b of 235 K.

Figure 2 shows a spectral energy distribution at centimeter wavelength. The SED contains both of the low-resolution ATCA data tracing the extended ($\sim 1''$) radio jet (Motogi *et al.* 2013) and high-resolution JVLA data tracing the newly detected compact emission. We found that the former could be modeled by a typical radio jet emission with a positive spectral index (α; $S(\nu) \propto \nu^\alpha$) of 0.5. The JVLA data, on the other hand, clearly showed α of ~ 2, suggesting the optically thick emission.

The relatively low T_b and slightly resolved source structure can exclude any possibility of a very compact HII region. For example, the observed flux of 3.5 mJy at 45 GHz corresponds a source size of only 18 milli-arcsecond in the case of optically thick HII region with the electron temperature of 10^4 K. Alternatively, such a low T_b and spectral index of 2 are naturally explained by the optically thick dust emission. The association of the 6.7 GHz CH_3OH maser, which is excited by warm dust emission (Cragg *et al.* 2005), is also consistent in this case. We, thus, suggest that the continuum traces warm dust in the innermost circumstellar system.

3.2. *6.7 GHz CH_3OH maser*

Figure 1 also presents the internal distribution of 30 bright CH_3OH maser spots (signal-to-noise ratio > 30) that have accurate relative positions compared to the scale of the maser distribution. Since it is difficult to directly compare the 45-GHz continuum position and maser distribution, due to the significant astrometric error in ATCA data ($\sim$400 mas), we superposed the maser distribution on the continuum image.
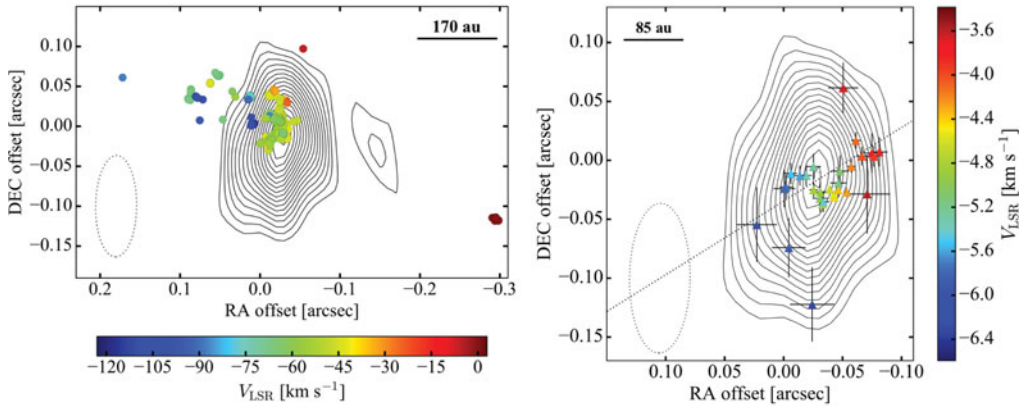
Figure 1. Left: The contours present JVLA 45-GHz continuum image, which are from 19 (3 σ) to 99% with step of 5% of the image peak flux (1.39 mJy beam^{-1}). Filled circles show VLBI map of the H$_2$O maser jet in Motogi *et al.* (2016) with a color indicating the LOS velocity (See the online color version). The coordinate origin is the phase tracking center, 17^{h}26^{m}01^s.59, -34°15′14″.90 (J2000.0). Right: Internal distribution of the 6.7 GHz CH$_3$OH masers. Filled triangle shows a position of each maser spot with a color indicating the LOS velocity (See the online color version). The maser map is superposed on the continuum image, assuming that the peak position of the 6-GHz continuum is identical to that of the 45-GHz continuum. The synthesized beam of JVLA is shown in lower left corner in both figures.
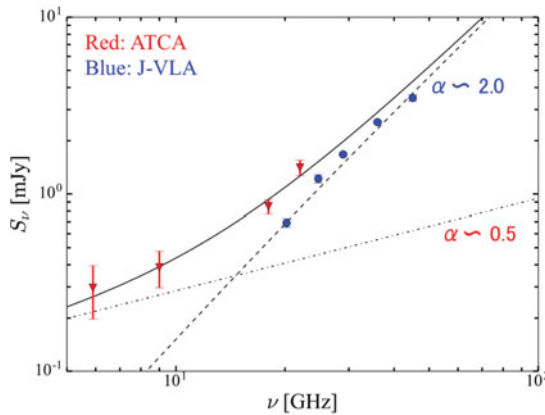

Figure 2. The centimeter SED between 6 – 45 GHz. Filled circles and triangles indicate high--resolution JVLA data and low-resolution ATCA data, respectively. The dotted and dash-dot lines show the best-fit model of the optically thick compact dust emission ($\alpha \sim 2.0$) and the extended radio jet ($\alpha \sim 0.5$), respectively.

The maser distribution in Figure 1 appears spiral-like rather than ring or linear shape, accompanied by systematic velocity gradient ($\pm$ 1.5 km s^{-1} over 0.15 arcsec). We have found that this velocity structure is well explained by infall streams which fall down to the equatorial plane of the inner accretion disk, along the point symmetric trajectory. Figure 3 shows the schematic view of our parabolic infall model with the best-fit result (see Motogi *et al.* 2017 for details). We note that recent ALMA observations towards a low mass class 0 object have found that similar non-axisymmetric streams fall down onto the edge-on accretion disk along a parabolic orbit (Yen *et al.* 2014).

The infall streams reach the equatorial plane at the landing radius (R_0) of 16 au in the best-fit case. This is clearly smaller than that of typical accretion disks in high mass
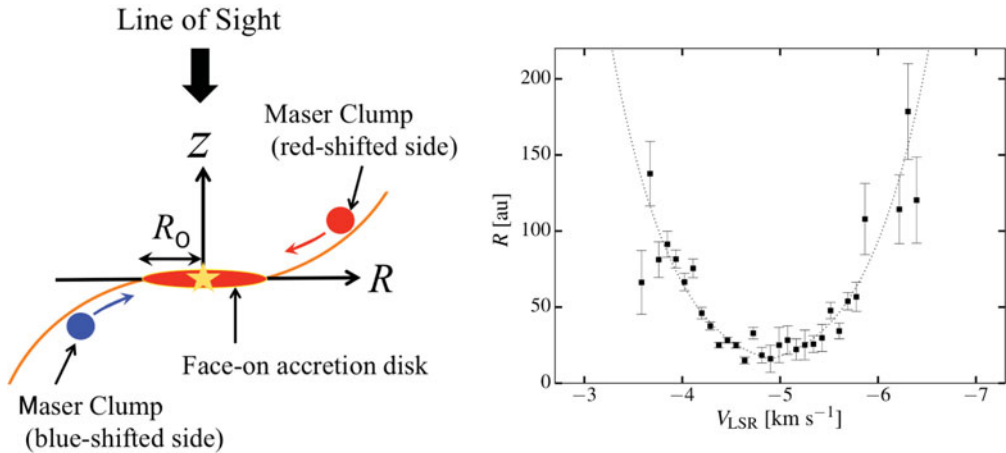
Figure 3. Left: Schematic view of the parabolic infall model. Two filled circles indicates a blue-shifted and red-shifted infalling CH_3OH maser clumps, respectively. The LOS is along the Z direction. Right: Distance-velocity diagram of the CH_3OH masers. A dotted line indicates the best-fit result of our parabolic infall model (see Motogi *et al.* 2017 for details). The x and y axes show LOS velocities and a projected distances of maser spots with respect to the dynamical center that was determined by the model fitting, respectively.

star-formation (Beltrán & de Wit 2016, and references therein). This fact indicates that the initial angular momentum in G353 is very small, or the CH_3OH masers selectively trace accreting material that has a small angular momentum.

Our model also expects that the streamline is quasi-radial ($Z/R < 10$ per cent) even at the outer region ($R \sim 200$ au). This fact indicates that centrifugal force is basically negligible, although the head-tail like distribution of the blue-shifted masers in Figure 1 may imply non-zero angular momentum. Such an infall-dominated motion of the class II CH_3OH maser at 100-au scale has actually been detected in a VLBI study by Goddi, Moscadelli & Sanna (2011).

3.3. *Conclusion*

Our results suggested the presence of the innermost (~ 100 au) dusty and infall-dominated accretion system in G353. However, the origin of such a specific structure is still an open question. The infall model will be verified by thermal continuum and line observations in the higher-resolution (~ 10 mas), resolving a face-on disk, infall streams, etc. This will be done by our ALMA long baseline project. In addition, infall motion of the CH_3OH maser itself will be directly examined by on-going proper motion measurements by VLBA. 3D velocity field will also constrain an accretion rate within 100 au, combined with mass information obtained by ALMA.

References

Beltrán, M. T. & de Wit, W. J. 2016, *A&A Rv*, 24, 6
Caswell, J. L. & Phillips, C. J. 2008, *MNRAS*, 386, 1521
Cragg, D. M., Sobolev, A. M., & Godfrey, P. D. 2005, *MNRAS*, 360, 533
Goddi, C., Moscadelli, L., & Sanna, A. 2011, *A&A*, 535, L8
Motogi, K., Sorai, K., Niinuma, K., *et al.* 2013, *MNRAS*, 428, 349
Motogi, K., Sorai, K., Honma, M., *et al.* 2016, *PASJ*, 68, 69
Motogi, K., Hirota, T., Sorai, K., *et al.* 2017, *ApJ*, 849, 23
Yen, H.-W., Takakuwa, S., Ohashi, N., *et al.* 2014, *ApJ*, 793, 1